

A new, high sensitivity laser vibrometer

J.R. BAKER, R.I. LAMING, T.H. WILMSHURST, N.A. HALLIWELL

This paper introduces a new design of laser vibrometer which allows high sensitivity, non-contact measurement of normal-to-surface target motion. The design includes use of a retro-reflective tape covered PZT-element to remove the sign ambiguity in surface velocity, which is inherent in the form of Doppler detection used in laser vibrometers. Utilization of this element offers the potential for a compact, cost effective design, suitable for portable, on-site use in engineering situations.

KEYWORDS: vibrometers, laser Doppler velocimetry, PZT

Introduction

Since the advent of the laser, optical metrology has provided vibration engineers with data formerly considered unobtainable, for example from hot, light or rotating target surfaces, where use of traditional contacting transducers is precluded. Additional problems include the time-consuming task of transducer attachment when vibration surveys are required, and at high frequencies, contact resonance phenomena associated with the means of transducer connection.

The application of laser Doppler velocimetry¹ (LDV) to this problem has produced a range of laser vibrometers²⁻⁴, a number of which are now commercially available. Laser vibrometer operation relies on detection of the Doppler shift in laser light backscattered from the target surface, which, when mixed with a reference beam on a photodetector surface, produces a time-resolved vibrometer output proportional to the modulus of the target surface velocity vector. In practice, both the amplitude and sign of velocity are required and thus the direction ambiguity problem, inherent in this form of Doppler detection, must be overcome. This is achieved by frequency shifting the reference beam, thus providing a carrier frequency which is subsequently modulated by any target surface motion¹. Commercial systems differ primarily in the frequency shifting mechanism they employ, for example Bragg cells³, rotating diffraction gratings⁴ or rotating scattering discs², leading to a range of

laser vibrometers varying in expense, robustness, bulk, ease of use and portability.

For practical vibration measurements, it is erroneous to specify a laser vibrometer noise floor without specific reference to the target surface dynamics⁵. Consequently, the choice of laser vibrometer system is dictated by its intended application. For vibrometer measurements on large, heavy structures, for example for modal analysis applications, ultimate sensitivity is of particular importance since at frequencies of interest, typical velocity levels are often extremely low. Hence there is a real need for a laser transducer that is compact, robust, user friendly and cost effective compared with systems intended for more general use.

This paper describes a novel form of laser vibrometer developed using a demodulation scheme for fibre optic sensors suggested by Dandridge et al⁶. It is intended for high sensitivity measurements, where it can be reasonably assumed that the effect of the laser speckle pattern dynamics generated by the target surface can be ignored⁵. The system employs a piezoelectric (PZT) element as a reference beam frequency-shifting element and as such, is compact, robust, self-aligning and cost-effective relative to other laser vibrometers. The practical system included the following modifications.

- The vibrometer uses diffuse reflection from the optically rough surface of the PZT element, compared with the mirror-like surfaces used in the Dandridge system. This enables the instrument alignment to be far less critical and the vibrometer significantly more robust.
- The PZT element used is driven at a resonant frequency of 0.75 MHz compared with 50 kHz, which allows for a maximum peak velocity of -34.5 dB reference 1 ms^{-1} , compared with

JRB is at the Institute of Sound and Vibration Research and RIL and THW are in the Department of Electronics and Computer Science, University of Southampton, Highfield, Southampton, SO9 5NH, UK. NAH is in the Department of Mechanical Engineering, Loughborough University of Technology, Loughborough, Leicestershire, LE11 3TU, UK. Received 25 September 1989. Revised 16 February 1990.

-58 dB, and an associated increase in the instrument dynamic range.

- The optical geometry and opto-electronics have been optimized for use with diffusely reflecting target surfaces as are normally encountered on engineering components.

Measurements have shown that the noise floor is comparable with that of an accelerometer for the same measurement situation and approaches the theoretical electronic noise limit when the target surface is stationary.

Physics of operation

Utilizing the Michelson interferometer configuration shown in Fig. 1, the laser beam is divided into two components which are incident on the target and reference surface respectively. Light is back-scattered from each surface on to a photodetector, producing a detector output current i_d , given by

$$i_d = \alpha [I_P + I_T + 2(I_P I_T)^{1/2} \cos \theta] \quad (1)$$

where I_P and I_T are the reference and target beam scattered light intensities, α is a photodetector response term and θ the phase difference term due to a path-length imbalance. With reference to Fig. 1, this phase term is directly proportional to any relative change ($L_1 - L_2$) in position of either surface, such that

$$\theta = 2k\beta + \theta_0 \text{ (rad)} \quad (2)$$

where $\beta = (L_1 - L_2)$, k is the wave-number of laser light and θ_0 the initial phase difference. As noted in the introduction, using the optical geometry shown in Fig. 1, it is not possible to determine the target surface velocity direction, and the reference beam is frequency pre-shifted to provide a carrier frequency in the photodetector output, which movement of the

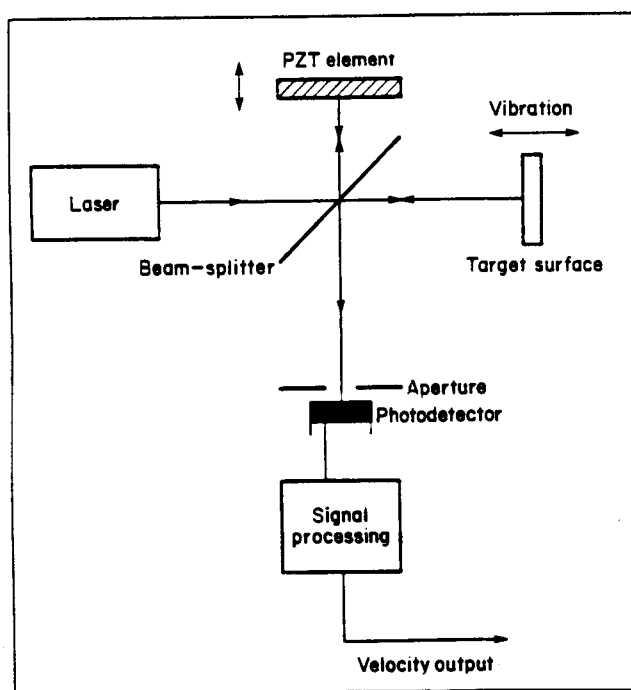


Fig. 1 Laser vibrometer optical configuration

target then modulates¹. Tracking the carrier frequency provides a time-resolved analogue output of the target surface velocity. In the proposed system, the reference light is frequency shifted by driving the reference surface, that is, a PZT element, sinusoidally such that

$$L_1 = A \sin \omega_P t \quad (3)$$

where A and ω_P are the PZT displacement amplitude and frequency respectively. For sinusoidal target motion, the time-varying detector current $i_d(t)$ will then be

$$i_d(t) = \alpha [I_P + I_T + 2(I_P I_T)^{1/2} \cos(2k[A \sin \omega_P t - B \sin \omega_T t] + \theta_0)] \quad (4)$$

where B and ω_T are the target displacement amplitude and frequency respectively. This equation reduces to

$$i_d(t) = C_1 [1 + C_2 \cos(\theta_P \sin \omega_P t - \theta_T + \theta_0)] \quad (5)$$

where

$$\theta_P = 2kA; \quad \theta_T = 2kB \sin \omega_T t;$$

$$C_1 = \alpha(I_P + I_T);$$

$$C_2 = \frac{2(I_P I_T)^{1/2}}{I_P + I_T}$$

Expanding (5) in terms of Bessel functions

$$i_d(t) = C_1 \left[1 + C_2 \cos \theta_T \left\{ J_0(\theta_P) + 2 \sum_{n=1}^{\infty} J_{2n}(\theta_P) \cos(2n\omega_P t) \right\} + C_2 \sin \theta_T \left\{ 2 \sum_{n=0}^{\infty} J_{2n+1}(\theta_P) \sin((2n+1)\omega_P t) \right\} + C_2 \cos \theta_0 \right] \quad (6)$$

Therefore in contrast with the majority of LDV systems, the photodetector output contains PZT element-generated carrier frequency terms at ω_P and higher order harmonics, each of which the target surface will frequency modulate. It will now be shown how the target surface velocity information can be retrieved from this form of signal by selecting specific carrier frequencies at ω_P and $2\omega_P$.

With reference to Fig. 2, the photodetector output is initially band-pass filtered to produce signals $i_{\omega_P}(t)$ and $i_{2\omega_P}(t)$ given by

$$i_{\omega_P}(t) = 2C_1 C_2 J_1(\theta_P) \sin(\omega_P t) \sin(\theta_T) \quad (7a)$$

$$i_{2\omega_P}(t) = 2C_1 C_2 J_2(\theta_P) \cos(2\omega_P t) \cos(\theta_T) \quad (7b)$$

As shown in Fig. 2, phase-sensitive detectors⁷ with reference inputs at frequencies ω_P and $2\omega_P$ respectively then give outputs

$$x = GC_1 C_2 \sin \theta_T; \quad y = GC_1 C_2 \cos \theta_T \quad (8)$$

where G is the effective channel gain, which incorporates $J_1(\theta_P)$ and $J_2(\theta_P)$ and is adjusted to be the same for each channel. Practical measurements

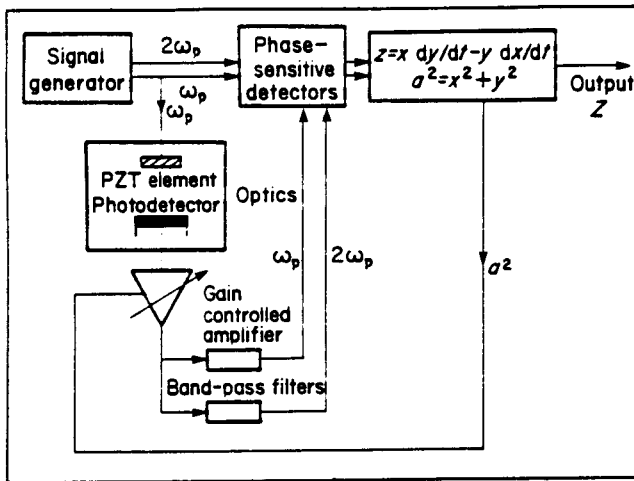


Fig. 2 Schematic diagram of signal processing electronics

have shown that for accurate demodulation, x and y must be precisely balanced using potentiometers. A system of analogue multipliers and differentiators³ then gives the outputs

$$z = x \frac{dy}{dt} - y \frac{dx}{dt}, a^2 = x^2 + y^2 \quad (9)$$

where

$$z = (GC_1C_2)^2 \frac{d\theta_T}{dt} \quad (10)$$

$$a^2 = (GC_1C_2)^2 \quad (11)$$

Here z is proportional to $d\theta_T/dt$ and hence represents the target velocity. However, the term C_1C_2 is dependent on the intensity of light scattered from the target and this will vary with measurement position. As shown in Fig. 2, this effect is overcome by employing an automatic gain control system, whereby G is adjusted to keep a^2 constant for varying C_1C_2 and thus maintain the term $(GC_1C_2)^2$ in (10) constant also.

Comparison with other transducers

The prototype vibrometer has a measured dynamic range of approximately 100 dB over the vibration frequency range 0 to 10 kHz. A range of sensitivity settings in the demodulator circuit are employed to improve the signal-to-noise ratio for varying velocity amplitudes, producing a stationary surface noise floor level of approximately -150 dB reference 1 m s^{-1} at 1 kHz. The -50 dB upper velocity limit of the vibrometer is determined by the bandwidth of the input band-pass filters at ω_p and $2\omega_p$.

Fig. 3 compares a spectrum of the vibrometer output with that of an accelerometer for the same measurement situation. A 2 mW He-Ne laser was used, producing an incident intensity target beam of 1 mW. The beam was directed on to the top of an accelerometer which was being driven by an electrodynamic shaker at 190 Hz. A small piece of retro-reflective tape was placed on the accelerometer to ensure sufficient intensity in the backscattered light collected by the photodetector.

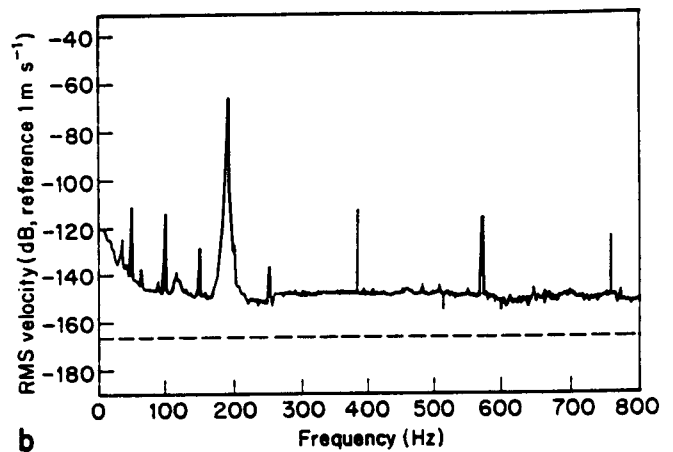
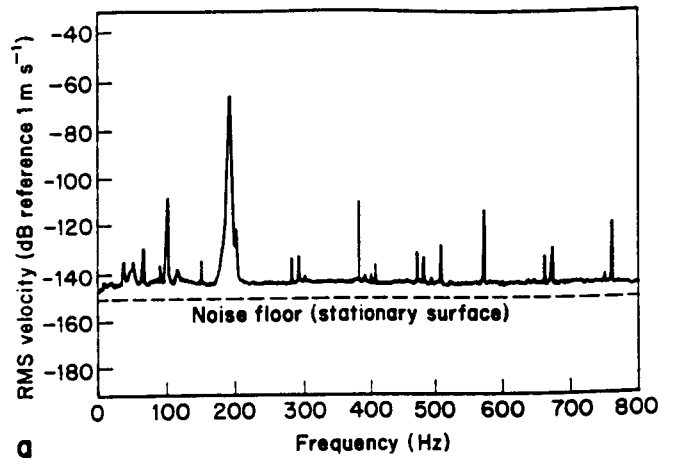


Fig. 3 Comparison of the response of (a) the laser vibrometer and (b) an accelerometer. 100 averages; 800 Hz bandwidth, 1 Hz resolution

The spectra shown in Fig. 3 contain 100 averages with a frequency resolution of 1 Hz. Excellent agreement is obtained and for this measurement a minimum detectable level for the vibrometer is shown to be better than -140 dB. This compares favourably with the most sensitive setting of the accelerometer at -145 dB. Measurements taken on a stationary surface produced noise floor levels from the vibrometer and accelerometer of -150 and -165 dB respectively. This difference in noise floor level is due to electronic noise in the vibrometer demodulation scheme and can be improved by reducing the measurement frequency bandwidth.

From Fig. 3 it can be seen that the vibrometer is able to make velocity measurements down to 0 Hz, whereas below approximately 60 Hz, the integrated accelerometer output suffers from low frequency noise. The spurious twin peaks in the vibrometer spectrum at a level of approximately -130 dB originate in the demodulation electronics, and work is continuing to remove them. It should also be noted that measurements made on a target undergoing in-plane or tilt motion as well as normal-to-surface vibration, will generate spurious signal peaks in the vibrometer output spectrum at the motion frequency and its harmonics⁵.

Inclusion of a semiconductor diode laser into the

laser vibrometer will produce a probe head considerably smaller than other laser vibrometer systems, offering ease of use and significant time savings when many vibration measurements are required.

Conclusions

A practical, high-sensitivity laser vibrometer is described in which a PZT element is employed to generate the reference beam frequency shift. Use of this device in conjunction with a solid-state laser diode offers the potential for an extremely compact, cost-effective transducer. The design is intended for use in modal analysis/vibration survey applications where rapid measurement of many points is required and target velocity levels are low. When the effects of target surface speckle dynamics can be neglected, a noise floor approaching that of a commercial accelerometer is achieved.

References

- 1 Durst, F., Melling, A., Whitelaw, J.H. 'Principles and practice of laser-Doppler anemometry'. Academic Press (1981)
- 2 Pickering, C.J.D., Halliwell, N.A., Wilmshurst, T.H. 'The laser vibrometer: a portable instrument'. *J Sound Vib.* 107 (3), (1986) 471-485
- 3 Bucchave, P. 'Laser Doppler vibration measurements using variable frequency shift'. *DISA Inf.* 18, (1975) 15-20
- 4 Oldengarm, J., Von Krieken, A.H., Raterink, H. 'Laser Doppler velocimeter with optical frequency shifting'. *Opt Laser Technol.* 5, (1973) 249-252
- 5 Rothberg, S.J., Baker, J.R., Halliwell, N.A. 'Laser vibrometry: pseudo-vibrations'. *J Sound Vib.* 135 (3), (1989) 516-522
- 6 Dandridge, A., Tveten, A.B., Giallorenzi, T.G. 'Homodyne demodulation scheme for fiber optic sensors using phase generated carrier'. *IEEE J Quant Elec.* QE-18 (10), (1982) 1647-1653
- 7 Wilmshurst, T.H. 'Signal recovery from noise in electronic instrumentation'. Adam Hilger (1985) Chapters 3 and 7
- 8 Wilmshurst, T.H., Rizzo, J.E. 'An autodyne frequency tracker for laser-Doppler anemometry'. *J Phys E: Sci Instrum* 7 (1974) 924-930

Articles for inclusion in future issues of *Optics & Laser Technology* include:

An achromatic collimator for a multi-window flight simulator
S.J. Dobson

Optical velocimeters for moving surfaces using gas and semiconductor lasers
P.Y. Belousov, Y.U. Dubnistshev, V.G. Meledin

Experimental analysis of the γ -ray ionization effects of a dc discharge CO₂ laser
I.B. Couceiro, R.A.D. Zanon, Y.K. Huang, C.A. Massone

Focal region isophote diagram as a calculating chart
K.R. Murali, Y.V.G.S. Murti

Electric field distribution in the incident medium of an oblique incidence reflector
J.C. Monga

Non-linear response of liquid crystal spatial light modulators
T.D. Hudson, D.A. Gregory

Various techniques for multiline operation of TEA CO₂ lasers
P.K. Gupta, U.K. Chatterjee

A semi-automatic method for measuring interferometry fringes: prototype design and first results
M. Buendía, C. Roldán, R. Cibrián, R. Salvador, M. Dolz, R. Belda, V. Herraéz, E. Ramón

A 20 W Cr³⁺, Tm³⁺, Ho³⁺: YAG laser
S. Imai, T. Yamada, Y. Fujimori, K. Ishikawa